


Research Article

Fracture Modeling of Deep Tight Sandstone Fault-Fracture Reservoir Based on Geological Model and Seismic Attributes: A Case Study on Xu 2 Member in Western Sichuan Depression, Sichuan Basin

Jitong Li ^{1,2}, Junlong Liu,² Hongde Chen,¹ Jianhua He,¹ Ruyue Wang,² Xupeng Shao,² and Xin Fang²

¹*Institute of Sedimentary Geology, Chengdu University of Technology, Chengdu, China*

²*Petroleum Exploration and Production Research Institute, SINOPEC, Beijing, China*

Correspondence should be addressed to Jitong Li; lijitong.syky@sinopec.com

Received 2 November 2022; Revised 5 May 2023; Accepted 25 May 2023; Published 14 June 2023

Academic Editor: Constantinos Loupasakis

Copyright © 2023 Jitong Li et al. This is an open access article distributed under the Creative Commons Attribution License, which permits unrestricted use, distribution, and reproduction in any medium, provided the original work is properly cited.

With significant geological reserves and high resource abundance, the Xujiahe Formation in the Western Sichuan Depression is considered a key target for natural gas exploration and development in continental clastic rocks within the Sichuan Basin. However, this formation remains underdeveloped. Critical to forming “sweet spots” of tight reservoir is the presence of fractures. Based on available data sources, including core samples, well logs, and outcrop data, we utilized a combination of geophysical and geological modeling techniques to clarify the characteristics of effective fractures in tight gas reservoirs. This allowed us to construct a geological model of a tight sandstone fault-fracture gas reservoir in the Xu 2 Member of the Xujiahe Formation located in the Xinchang area, which represents a fault-fracture reservoir formed by high-angle faulting-derived fractures and controlled by the S-N trending fault. With this model, a variety of seismic attributes, including likelihood and entropy, was used to predict the fault-fracture reservoir. Furthermore, geological information, well logs, and seismic attributes were integrated for characterizing the fractures of different scales. The cutoff on various attributes for characterizing the fault-fracture reservoir was defined, and the distribution of the fault-fracture reservoir was delineated. By using the geological modeling technique, the fracture model of the fault-fracture reservoir comprising natural fractures at different scales was built. This model provides further guidance for the exploration and development of the Xu 2 Member tight gas reservoirs in the Xinchang area and, as demonstrated by drilling results, has achieved remarkable effects in practice. This approach has shown good performance in characterizing fracture models. However, due to the complexity of fractures and the discrepancy between the scale of fractures and the scale that can be predicted by geophysical methods, there may still be some uncertainties associated with this method.

1. Introduction

Prediction of fractures is critical to the efficient exploration and development of tight oil and gas reservoirs [1–8].

Extensive effective fractures can significantly improve the porosity and permeability of tight reservoirs to make them favorable for hydrocarbon accumulation and subsequently economical “sweet spots” for exploration and development [9–16]. Geophysicists have used a variety of methods to detect the presence of fractures in the subsurface. These methods,

which rely on the physical properties of the subsurface, can be broadly divided into two categories: active and passive. Active methods involve the use of energy sources to generate signals which are then detected by instruments placed in the subsurface. Passive methods involve the use of natural signals which are detected by instruments placed in the subsurface. In addition to these methods, geophysicists have also used a variety of other techniques to detect fractures in the subsurface. All of these methods and techniques allow geophysicists to detect the presence of fractures in the subsurface, which can

then be used to predict the location and extent of subsurface fractures. However, the limitations of geophysical methods for predicting fractures mainly include the following two points: first, the types of data required by geophysical methods are limited. Typical data types include seismic wave velocity, vibration sensors, and ground detectors. These data types may themselves be insufficient information that could not be provided to fully describe the location, shape, and depth of the fracture.

The second is the limited resolution of geophysical methods, which can only detect sufficiently large fractures and may not be able to detect smaller fractures. Therefore, in practical applications, geophysical methods can only predict the approximate location, shape, and depth of fractures but cannot accurately predict the detailed information of fractures. Therefore, fracture prediction remains challenging due to the huge difference between the information scales (geologic data and seismic data) of fractures and the absence of a systematic fracture characterization method [17–19]. Also, fracture prediction may be ambiguous in the target, which is largely related to indefinite geological mode [20–23]. Under this background, the concept of a “fault-fracture reservoir” was proposed; thus, the focus of research shifts to the prediction of a large-scale effective fault-fracture reservoir [24–26]. The three-dimensional modeling and interpretation of fault-fracture reservoir enable the display of fracture distribution in space, providing better guidance for the exploration and development of tight gas reservoirs.

The origin of the fractures in the Xinchang Formation is closely related to the regional stresses that have affected the area. The Sichuan Basin is situated at the junction of the Yangtze and Tibetan Plateaus, which has resulted in the development of a complex stress field. The regional stresses are predominantly compressive, and they have acted in different directions and magnitudes over time. The folding processes that have affected the area have also played a significant role in the development of fractures in the Xinchang Formation. The Sichuan Basin has undergone several phases of folding throughout its history, and these have resulted in the formation of several sets of fractures. The folds in the area have a predominantly northeast-southwest orientation, and they have been influenced by the geometry of the Yangtze and Tibetan Plateaus. One of the main factors influencing the development of fractures in the Xinchang Formation is the orientation of the regional stresses relative to the folds in the area. The fractures tend to be oriented perpendicular to the maximum compressive stress direction, which is typically oriented northeast-southwest. This orientation is also consistent with the direction of the folds in the area. Another important factor is the lithology of the Xinchang Formation. The formation consists of alternating layers of sandstone, mudstone, and shale, which have different mechanical properties. The sandstone layers are more brittle than the mudstone and shale layers and are more likely to develop fractures under stress.

With the Xu 2 Member in the Xinchang area of the Western Sichuan Depression, the Sichuan Basin, as an example, the deep tight sandstone fault-fracture reservoir was predicted based on a geological model and seismic attributes.

Then, fracture modeling was conducted to define the geological model and the areal distribution of the fault-fracture reservoir. Finally, a three-dimensional geological model of the fault-fracture reservoir was established. The fracture modeling of fault-fracture reservoir addresses the problems in fracture prediction by traditional geophysical techniques which are difficult and inaccurate, and also provides guidance for the exploration and development of deep, tight sandstone gas reservoir and well deployment and target optimization.

2. Geological Setting

The Western Sichuan Depression in the western part of the Sichuan Basin is bordered to the north by the Micangshan piedmont, to the south by the Emei-Washan fault block, to the west by the Longmenshan nappe belt, and to the east by the central Sichuan uplift. It is an elongated depression trending NE-SW (Figure 1(a)) that covers an area of ca. 3.1×10^4 km². The Xinchang tectonic zone is located in the central north of Sinopec’s exploration area within the central Sichuan depression, with the exploration of ca. 3,000 km². To date, a total of 49 wells have encountered the Xu 2 Member (Figure 1(b)); thus, the data are relatively complete for tests. The study area is fully covered by a 3D seismic survey.

The upper part of T3X2 consists of gray, fine-grained lithic quartz sandstone, while the middle section consists of gray-black to black shale intercalated with light gray quartz sandstone. The lower part consists of shallow gray to light gray-white fine to medium-grained quartz sandstone, feldspathic lithic quartz sandstone, lithic quartz sandstone, and feldspar quartz sandstone interbedded with dark gray, light gray fine sandstone, and black shale of varying thickness. These beds are in contact with the underlying Xiaotangzi Formation. The production capacity of the Xu 2 Member in the Xinchang area is significantly influenced by the facies. Wells such as Xin 2, with the middle segment as the reservoir, and Lian 150, with the upper segment as the reservoir, are located in the main river channel during sedimentation, where the sand bodies are thick and the reservoir properties are good.

The Xinchang tectonic zone is a ENE-WSW-trending anticlinorium with multiple apexes. In its main part, there are two groups of faults. One group trends E-W, while the other trends S-N. In the Xiaquan area to the west, the fault is almost absent. Thrust faulting in this tectonic zone tends to be weakened as the burial depth decreases. The Xu 4 Member is remarkably less faulted than the Xu 2 Member. A total of 31 faults are recognized over the area with proven reserves. All of them are thrust faults and trends S-N, N-E, and E-W (Figure 2). Relatively, large-scale faults mainly trend S-N and are “Y”-shaped (Xin 851 and Xin 601 well blocks), imbricated, and parallel (Xin 5 well block) in the vertical direction.

In the Xu 2 Member, from bottom to top, 1 long-term cycle, 3 medium-term cycles, and 16–20 short-term cycles are identified, and the braided river delta facies is found, which can be divided into 3 subfacies and 6 microfacies. Underwater distributary channel deposits of the delta front dominate the study area. Reservoir porosity ranges from 0.44% to 16.38%, averaging 3.92%, indicative of a typical tight sandstone reservoir.

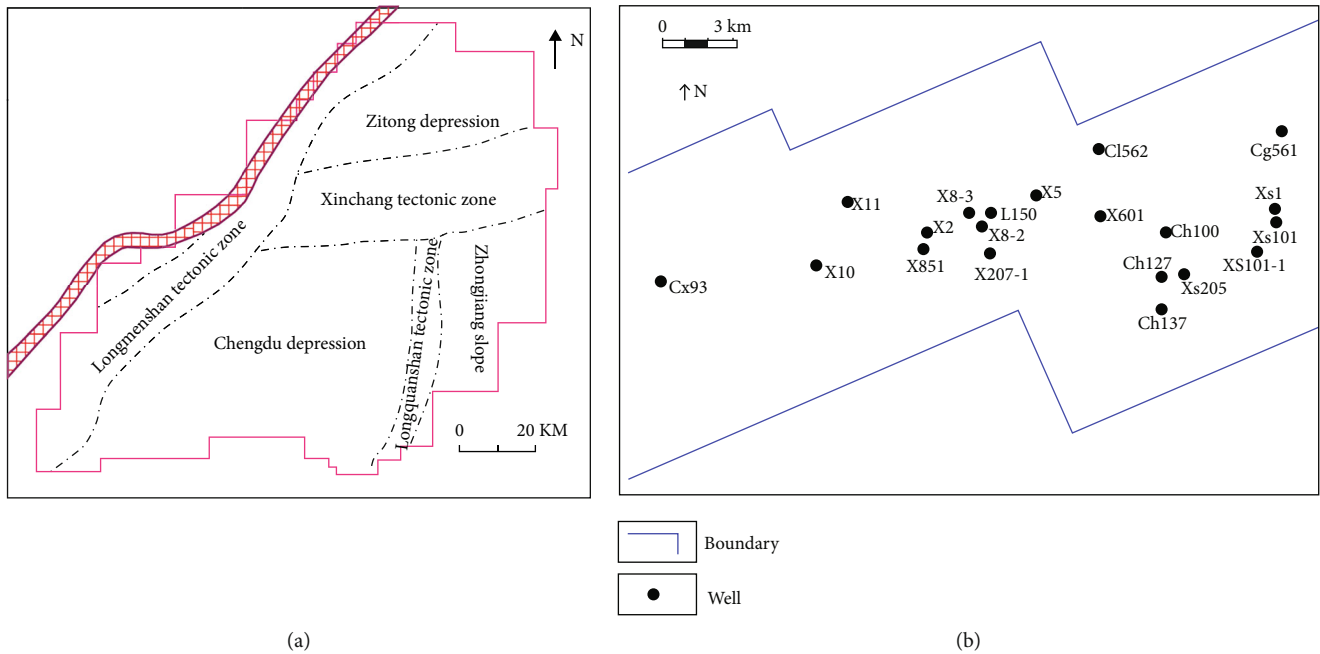


FIGURE 1: Structural location and key well distribution of the Xinchang area.

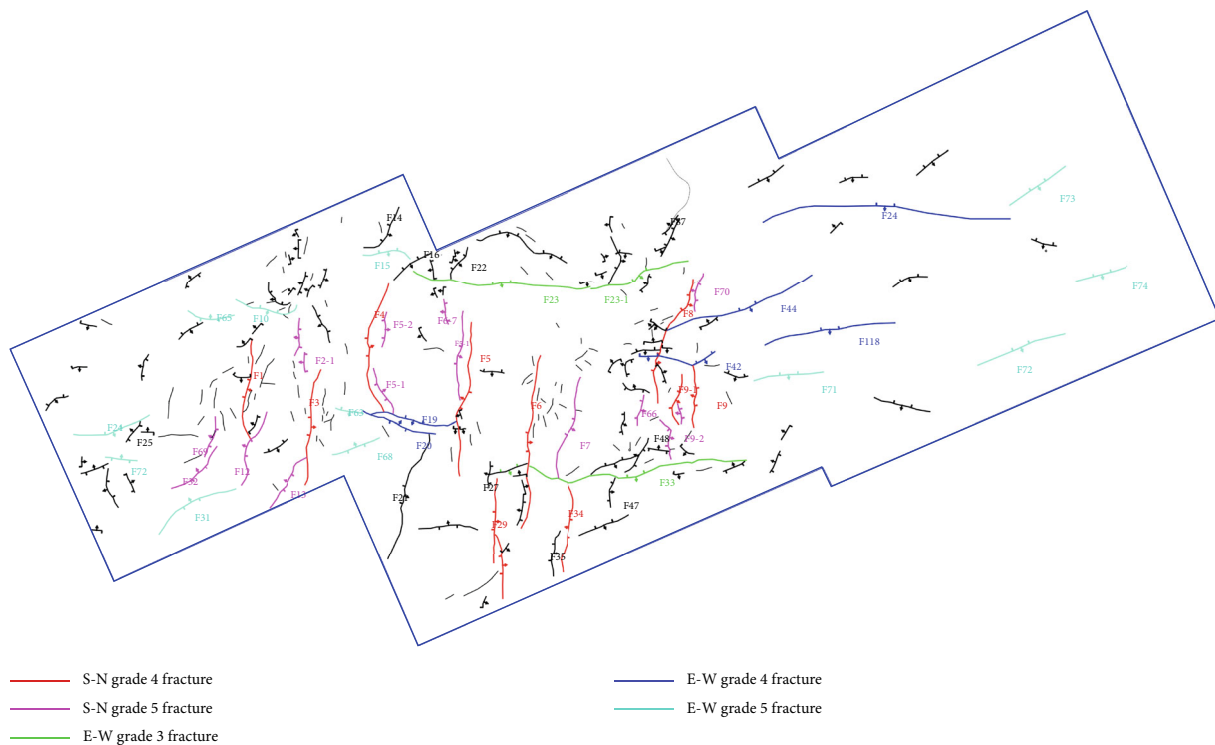


FIGURE 2: Structure outline map of TX22_top in the Xinchang tectonic zone.

3. Materials and Methods

3.1. *Concept of Fault-Fracture Reservoir.* A fractured reservoir is a kind of oil and gas reservoir in which the reservoir space is formed by the fracture network. It is a kind of complex reservoir, and its characteristics are the lack of porosity and permeability. A fractured reservoir is characterized by a

variety of fractures, including high-angle fractures, low-angle fractures, joints, faults, and other structures.

The concept of a “fault-fracture reservoir” was first put forward by Wang and Fan [27]. It refers to the geologic body containing fractures associated with faults and folds that constitute a three-dimensional pore-fracture network together with matrix pores. It was then applied to various

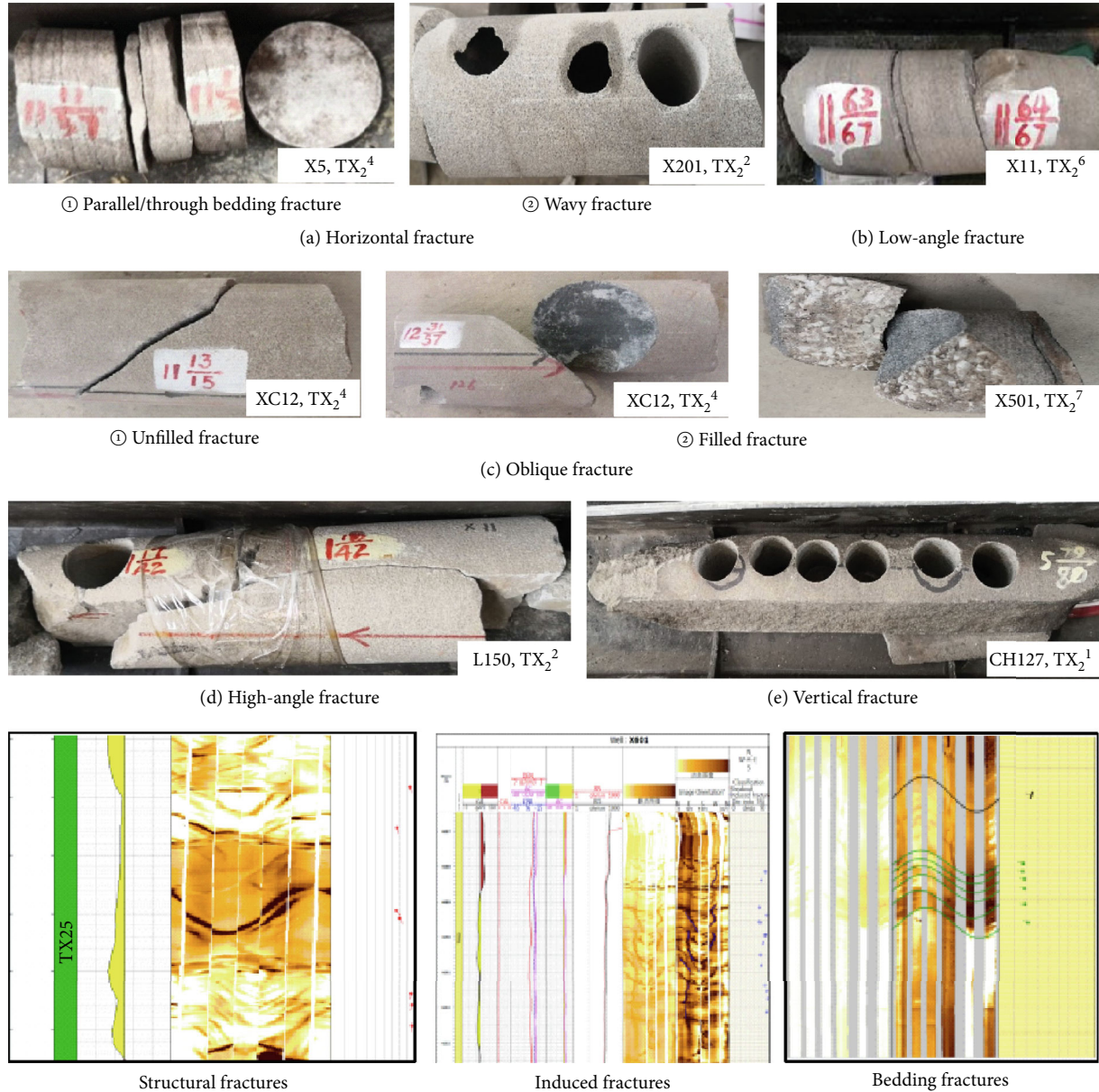


FIGURE 3: Type of fractures observed on cores from the Xu 2 Member in the Xinchang area.

regions to aid in exploration and development, with encouraging results reported. The Xinchang area is a key area that produces gas from tight sandstone in the Western Sichuan Depression. Yet, a critical limitation on further exploration and development in this area is that the distribution and development of fault-fracture reservoir remain unclear. A variety of data, including seismic, core, and image log, are integrated in this study to analyze the fault and fracture development. Then, the geological model that characterizes the fractures is utilized to constrain the seismic attribute-based prediction and description of the fault-fracture reservoir. Also, the geological modeling technique is utilized for interpreting and modeling the fault-fracture reservoir in order to provide guidance for the exploration and development of tight gas reservoirs in the Xinchang area.

4. Application and Discussion

4.1. Characteristics and Geological Model of Fault-Fracture Reservoir

4.1.1. Types and Characteristics of Effective Fractures

(1) *Types of Effective Fractures.* As observed on cores from 8 wells (Figure 3), five types of fractures are present in the Xu 2 Member in the Xinchang area, i.e., vertical fractures (dip angle $\geq 80^\circ$), high-angle fractures (dip angle of 60° – 80°), oblique fractures (dip angle of 30° – 60°), low-angle fractures (dip angle of 10° – 30°), and horizontal fractures (dip angle $\leq 10^\circ$). Generally, low-angle and oblique fractures are dominant, as 75%.

Horizontal fractures can be subdivided into parallel/trough bedding fractures and wavy fractures. Parallel/trough

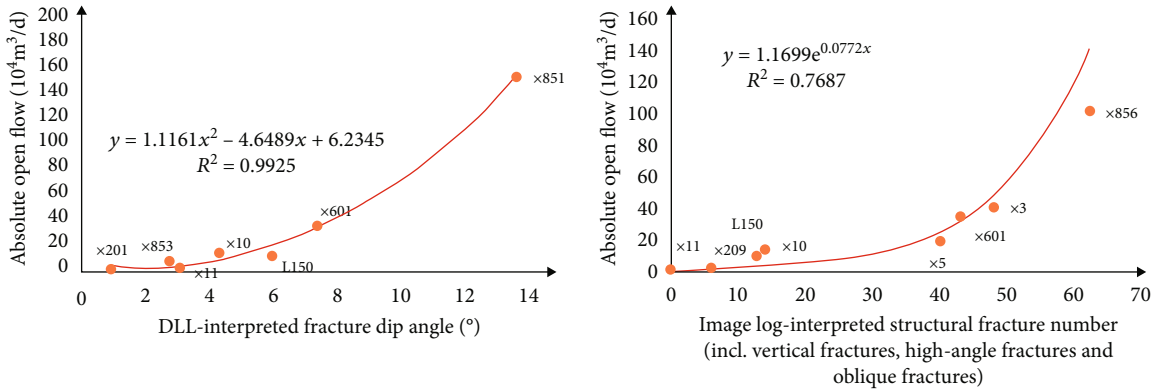


FIGURE 4: Crossplots of fracture and productivity for the Xu 2 Member, the Xinchang area.

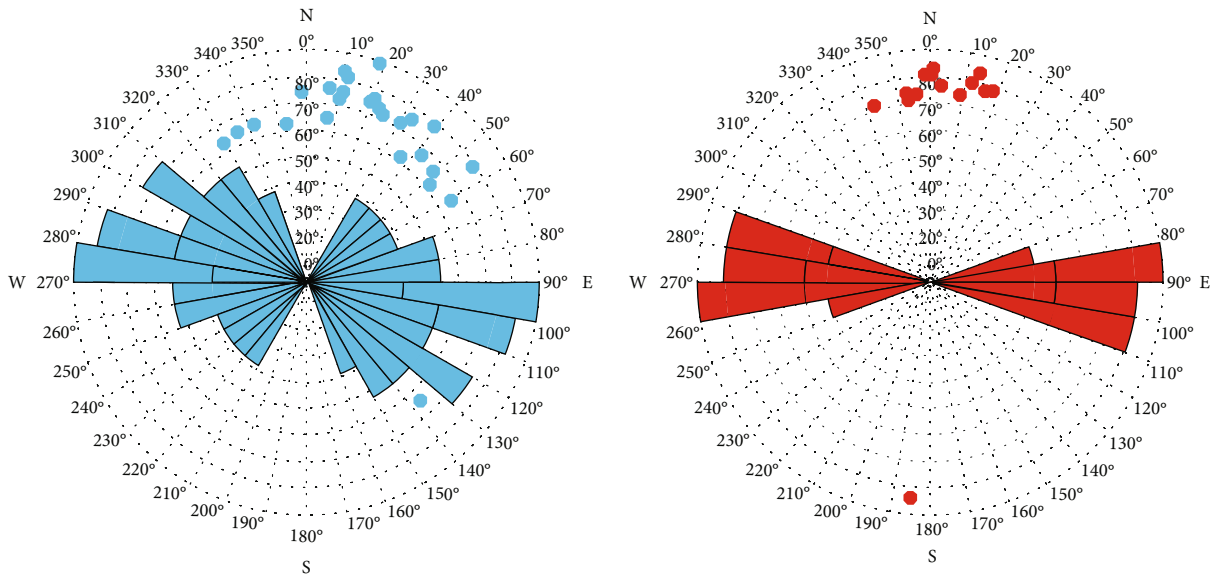


FIGURE 5: Rose maps showing the number and aperture of effective fractures in different sand groups of the Xu 2 Member, the Xinchang area (>60°).

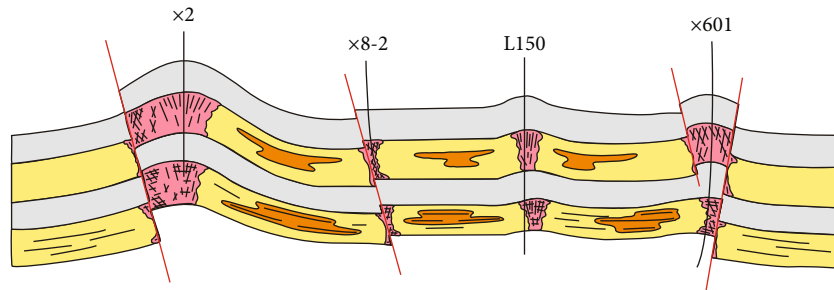


FIGURE 6: Geological model of the fault-fracture reservoir.

bedding fractures are mainly of depositional origin and correspond to the medium-coarse sandstone lithofacies in the “thick cake”/parallel bedding.

Low-angle fractures refer mainly to those oblique bedding fractures with a relatively low dip angle that crack along the original sedimentary interface.

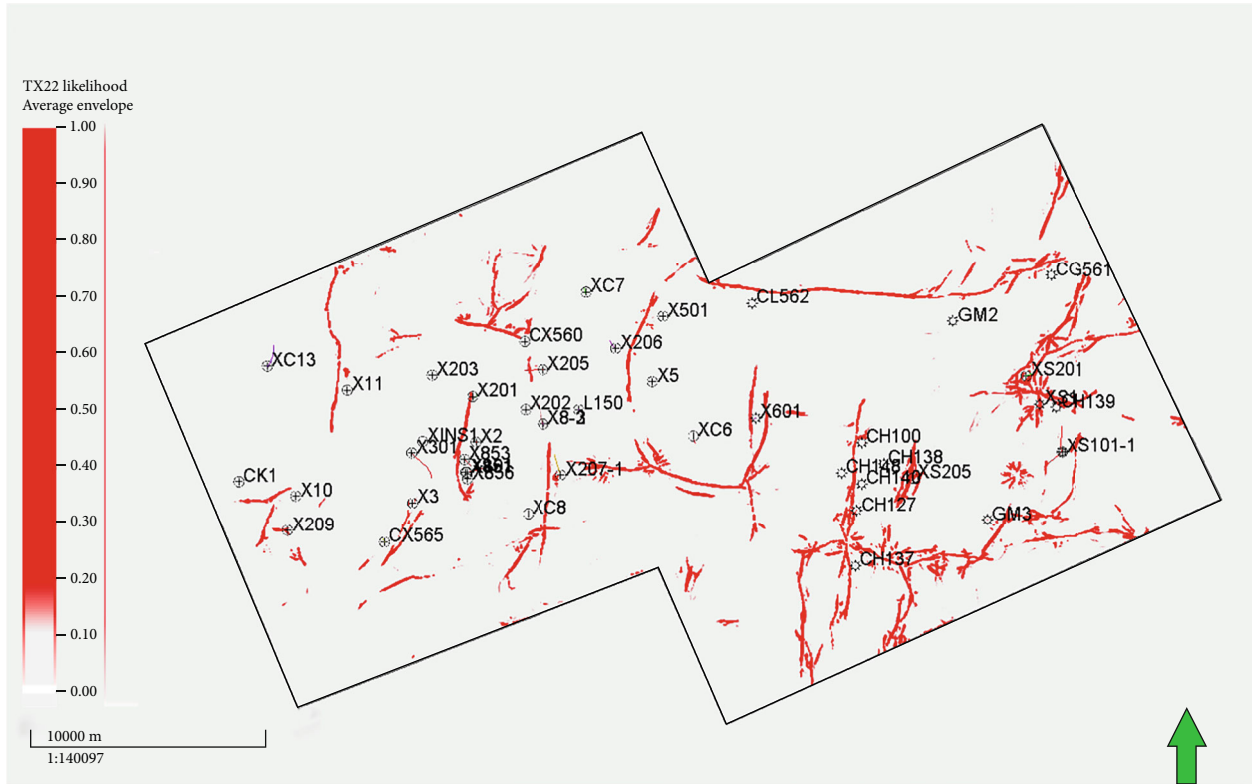


FIGURE 7: Maximum likelihood map of the Xu 2 Member in the Xinchang area.

Oblique fractures can be subdivided into unfilled fractures and filled fractures, depending on the degree of filling. Unfilled fractures were formed at a later stage, while filled fractures were formed at an early stage and then calcite-filled.

High-angle fractures refer mainly to fractures with a relatively high dip angle, which often marks high productivity in the Xu 2 Member in the Xinchang area.

Vertical fractures refer mainly to fractures that are nearly vertical, which also marks high productivity in the Xu 2 Member in the Xinchang area.

To find the right type of effective fractures that contribute most to productivity, based on well-log evaluation, 19 typical wells (including high-efficiency, low-efficiency, and nonefficiency wells) that penetrated the Xu 2 Member in the Xinchang area were selected for crossplot analysis of fracture parameters (e.g., image log-interpreted fracture density and dip angle, and conventional log-interpreted fracture porosity) extracted from the testing interval for vertical, high-angle, oblique, low-angle, and horizontal fractures and productivity parameters (e.g., absolute open flow and cumulative gas production) to determine how different types of fractures contribute to well productivity. The results (Figure 4) suggest that (1) the more abundant and higher angle the fractures, the higher the initial productivity of the gas well; and (2) the more abundant and dense the structural fractures with a dip angle $> 30^\circ$, the higher the initial productivity of the gas well.

As a summary, structural fractures with a dip angle $> 30^\circ$ (including vertical fractures, high-angle fractures, and obli-

que fractures) are considered effective fractures in the Xu 2 Member.

(2) *Characteristics of Effective Fractures.* Rose maps in Figure 5 show the effective fractures encountered by Wells Lian 150 (left) and Xin 601 (right). The characteristics of effective fractures are summarized on the basis of fracture characterization. The effective fractures principally trend E-W (Figure 5), perpendicular to the S-N trending faults (the fourth- to fifth-order faults) that control the productivity. Effective fractures are more developed in the hanging wall than in the footwall of faults. The closer to the faults, the more the high-angle fractures. Effective fractures are widespread in the TX₂², TX₂⁴, and TX₂⁵ sand groups, followed by TX₂³, TX₂⁶, and TX₂⁷.

4.1.2. *Geological Model of Fault-Fracture Reservoir.* According to the characteristics of effective fractures in the Xinchang area discussed above, a geological model of a fault-fracture reservoir can be built. It is found that the fault-fracture reservoir is controlled predominately by the S-N trending fault. The geological model of the fault-fracture reservoir in the Xu 2 Member in the Xinchang area is shown in Figure 6. Fractures in the fault-fracture reservoir are fault-dependent. Since faults have a “dual” structure, fractures are widespread within the sliding fracture zone and the induced fracture zone. Some fractures are controlled jointly by fault and fold. Both fault-dependent fractures and fold-dependent fractures are present. Similar to the fault-fracture reservoir, the fault-dependent

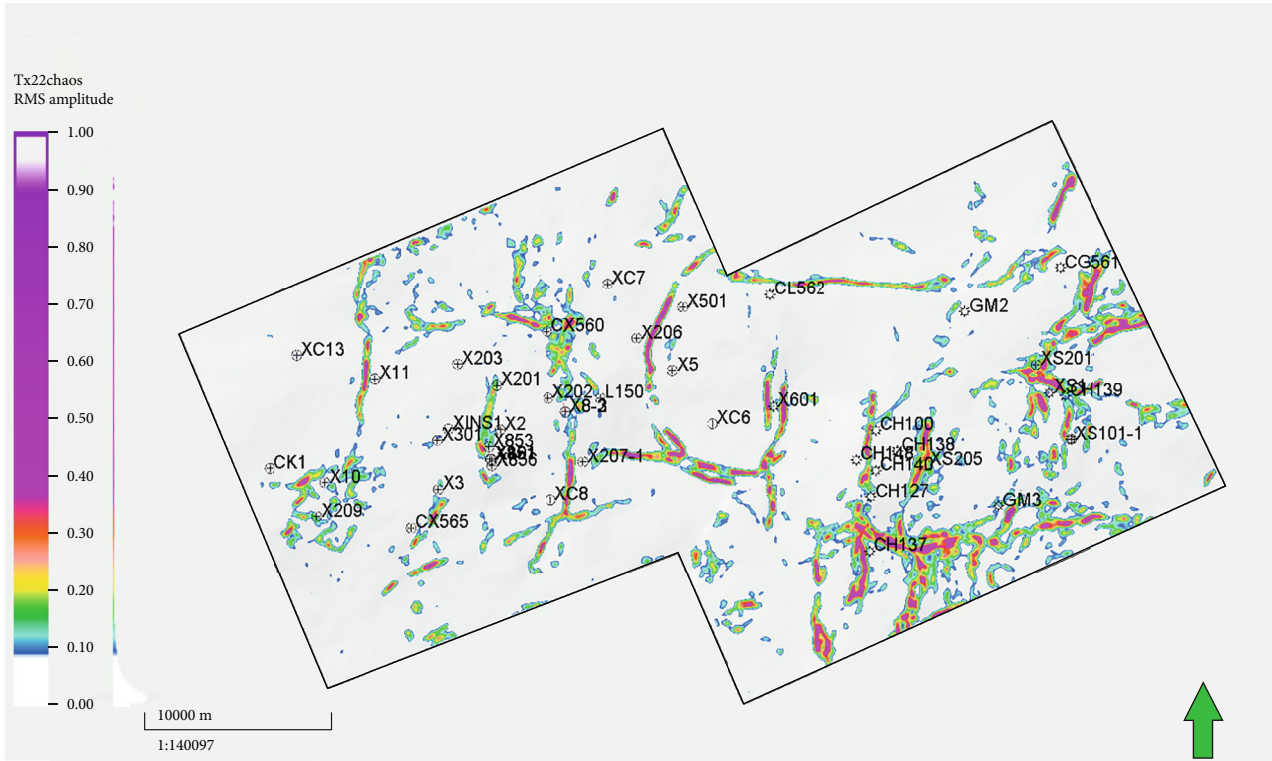


FIGURE 8: Entropy map of the Xu 2 Member in the Xinchang area.

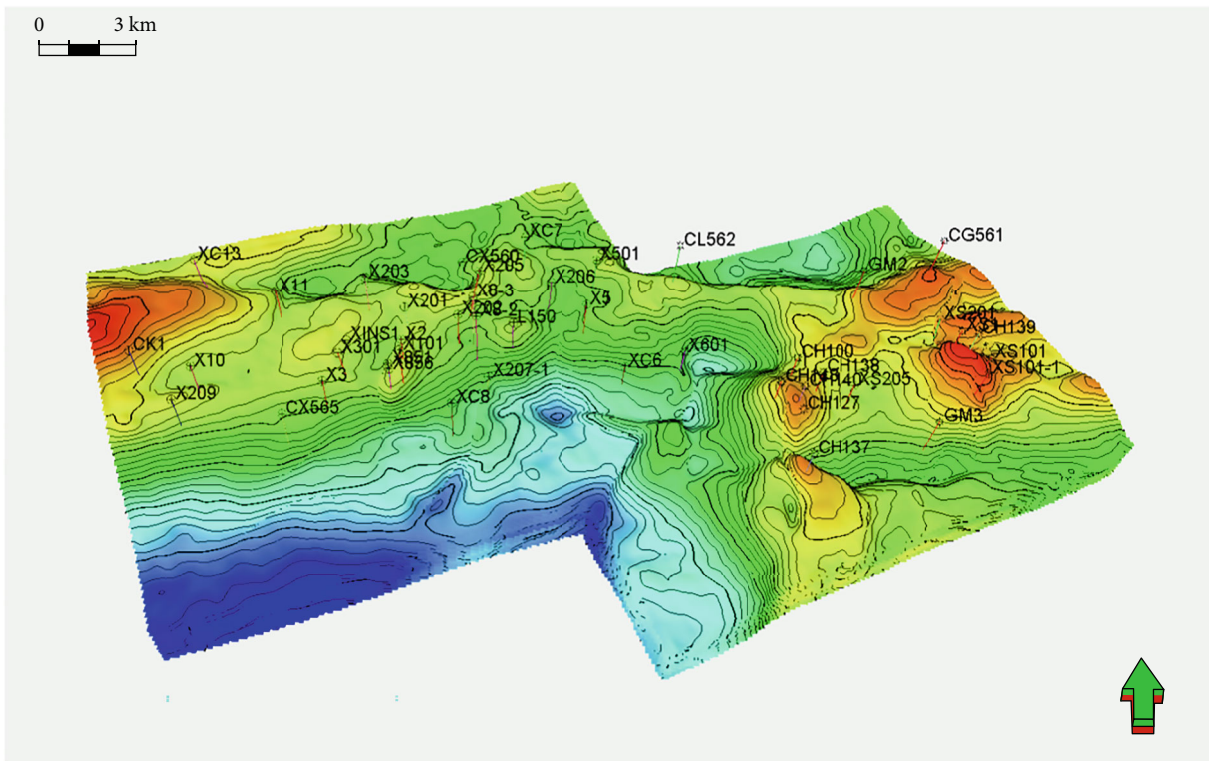


FIGURE 9: Horizon model of the Xu 2 Member in the Xinchang area.

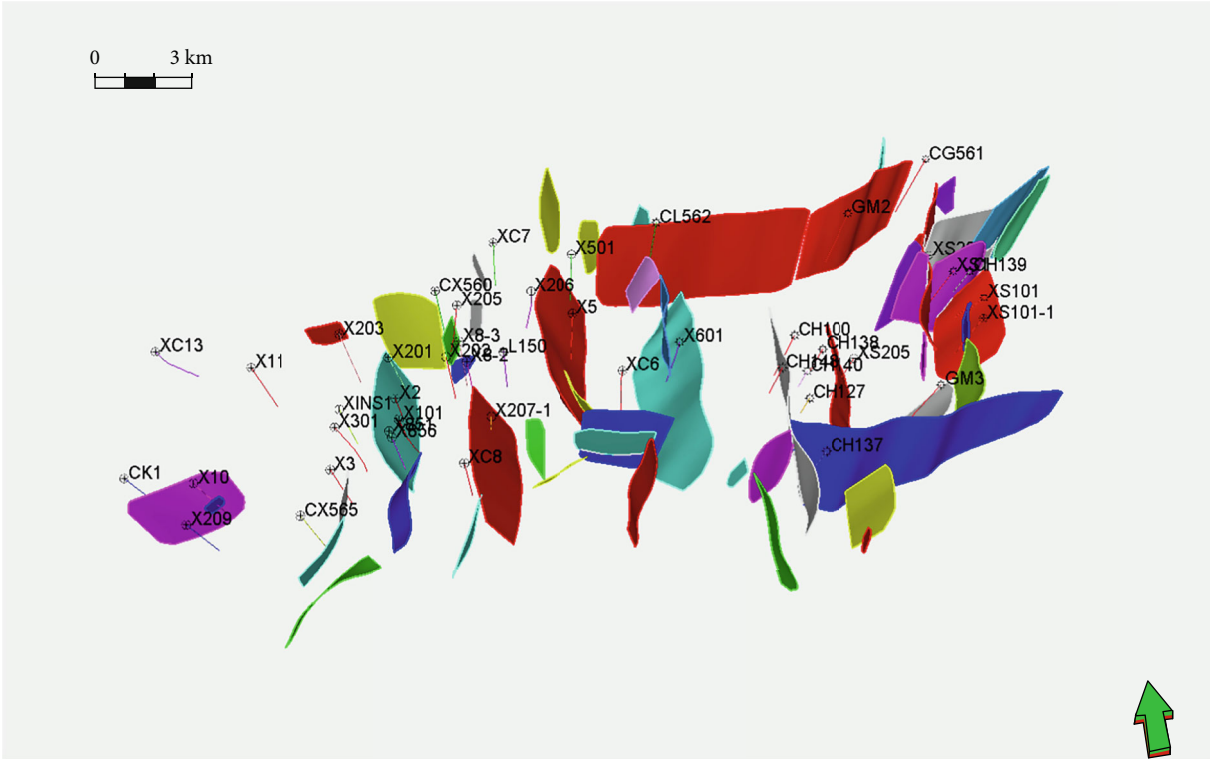


FIGURE 10: Fault model of the Xu 2 Member in the Xinchang area.

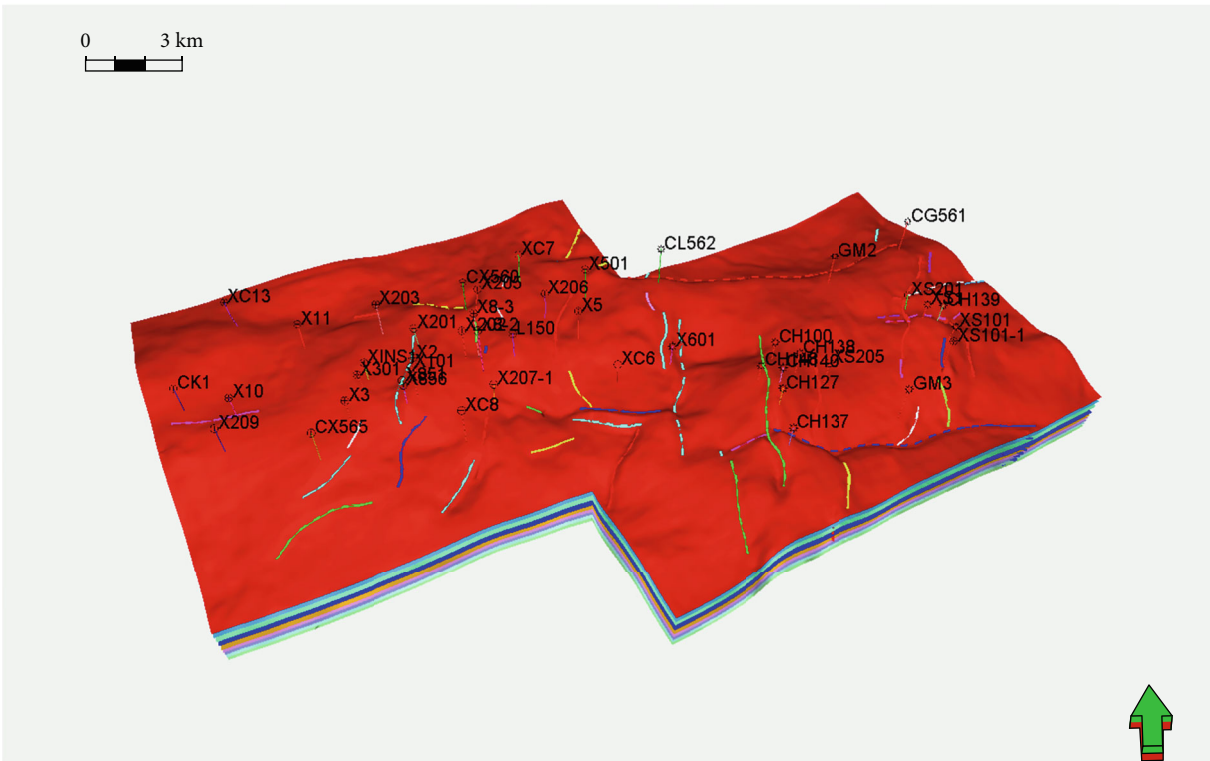


FIGURE 11: Structural model of the Xu 2 Member in the Xinchang area.

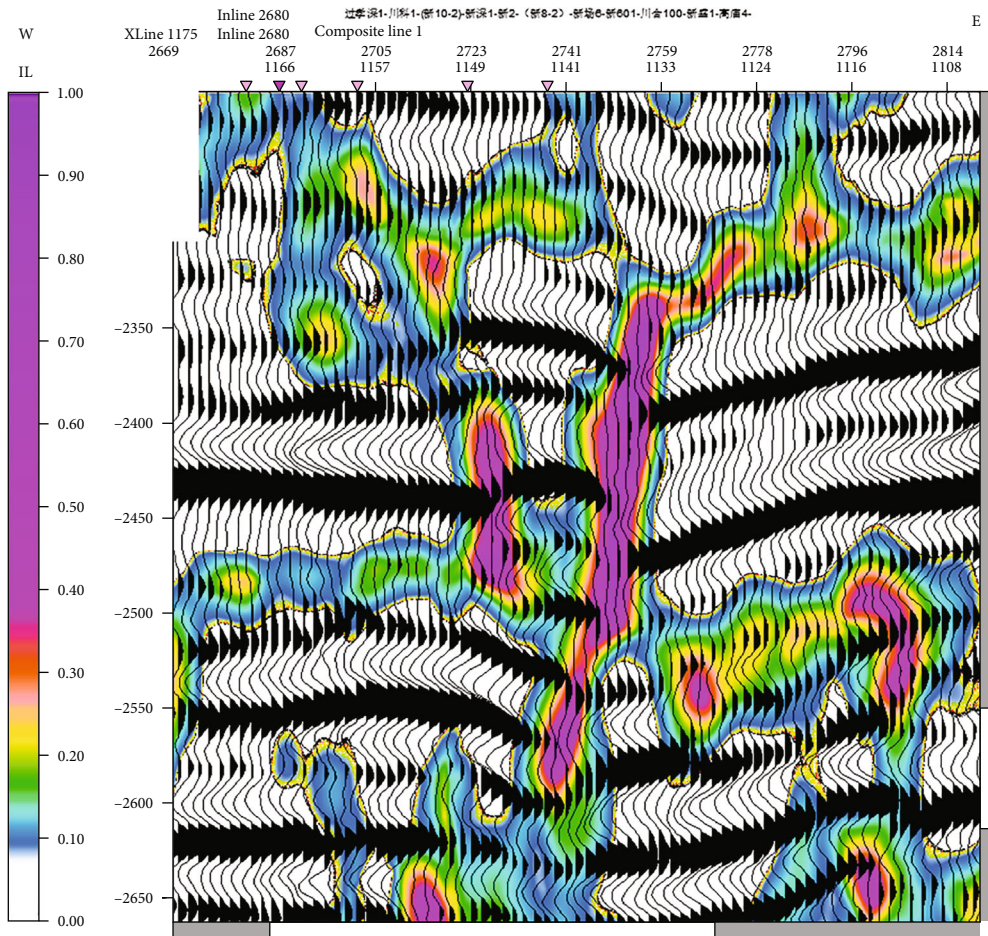


FIGURE 12: Entropy section showing the fault-dependent fractures in the Xu 2 Member, the Xinchang area.

fracture zone is centered at the sliding surface and controlled by the fault. In the Xinchang area, the fault-fracture reservoir in the Xu 2 Member is governed by fault-dependent fractures, while fold-dependent fractures are present in local areas and can provide an effective supplement to the fault-fracture reservoir in fracture prediction. The nearly E-W trending regional tectonic stress remains active since the Himalayan has significant control on the fault-fracture reservoir in the Xu 2 Member in the Xinchang area, resulting in the common presence of the nearly S-N trending faults in this area. In the proximity of these faults, fault anticlines are common. Also, nearly S-N or N-E trending anticlines are present locally. Fractures are often formed in the sliding fracture zone and induced fracture zone of the nearly S-N trending fault, the fault anticline in the hanging wall, and the hinge of the anticlinal structure in local areas. These fractures are nearly E-W, controlled by the nearly E-W regional tectonic stress field.

4.2. Multiattribute Prediction of Fault-Fracture Reservoir. The majority of faults in the Xu 2 Member in the Xinchang area has minor throws and is associated with numerous micro- and small-faults. It is therefore hard to distinguish internal structures of faults with seismic section only [28–30]. This paper makes an attempt to correlate the artificially interpreted faults and fracture zones observed on the

core and image log with the value of the likelihood attribute and GST- (gradient structure tensor-) based chaos (structure entropy) attribute. The analysis suggests that the likelihood attribute can reflect the sliding surface of the fault and the chaos (structure entropy) attribute can represent the sliding fracture zone and induced fracture zone. Likelihood can make the fault interpretation more objective (Figure 7). Overlapping the likelihood onto the chaos (structure entropy) section can help distinguish between the sliding fracture zone and the induced fracture zone. It is therefore possible to define the induced fracture zone and the sliding fracture zone as the development zone of fault-dependent fractures (Figure 8). In TX_2^2 , the development of fault-dependent fractures is controlled by the third- and fourth-order faults in the study area, alongside the fault strike. Generally, fractures are more developed in the eastern part than in the western part (Figure 7). In contrast, TX_2^4 hosts more densely spaced fractures than TX_2^2 , despite a similar extent that accommodates the fractures. This is deemed to be related to the fault scale in the sand group. Overall, fractures are present surrounding the fault zone.

4.3. Methodology for Fault-Fracture Reservoir Model Construction. As stated above, under the guidance of the geological model of fault-dependent fractures, geological

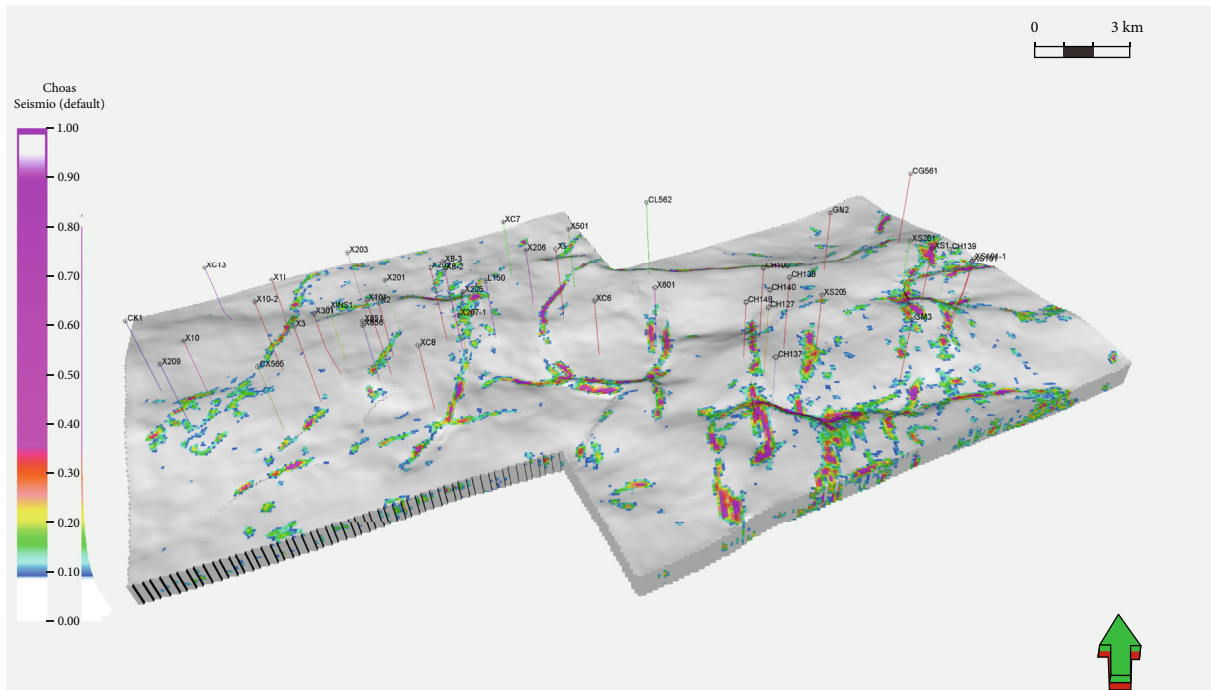


FIGURE 13: Constraint cube for the fault-dependent natural fracture distribution in the Xu 2 Member, the Xinchang area.

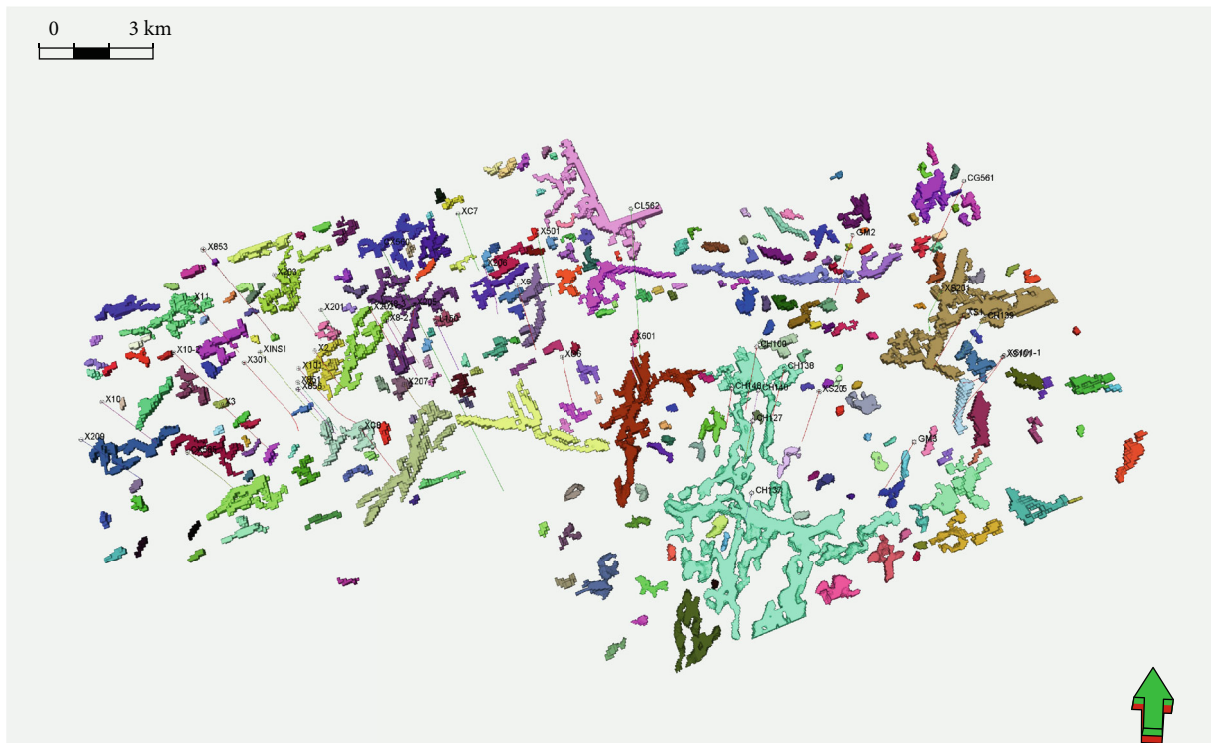


FIGURE 14: Fault-fracture reservoir model of the Xu 2 Member in the Xinchang area.

data, well log, and seismic attributes are integrated to characterize the fractures of different scales, and eventually the extent of the fault-fracture reservoir is delineated. Furthermore, the geological modeling technique is used to construct the fault-fracture reservoir model comprising natural fractures of different scales.

4.3.1. Construction of Structural Model. Structural modeling is the basis for building the fault-fracture reservoir model, including the stratigraphic model and the fault model.

Data sources for the stratigraphic model include seismic interpretation and well-based geological stratification. The first step is to obtain the seismic-interpreted horizon data

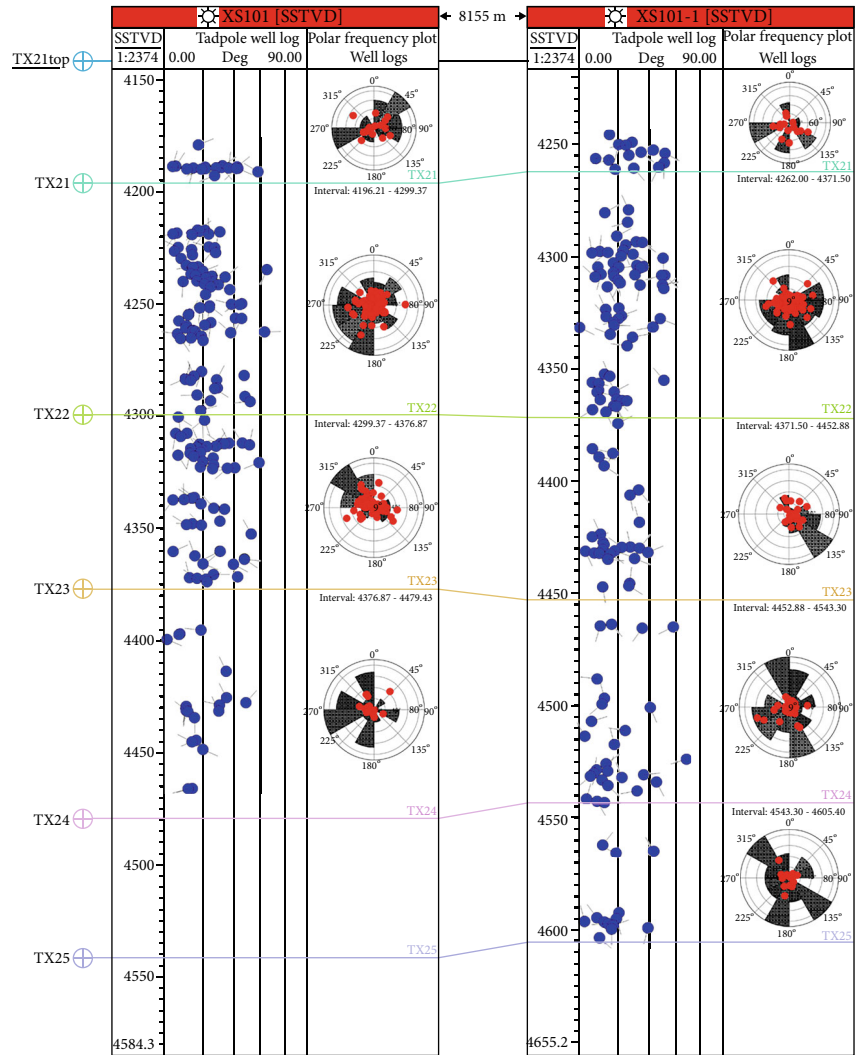
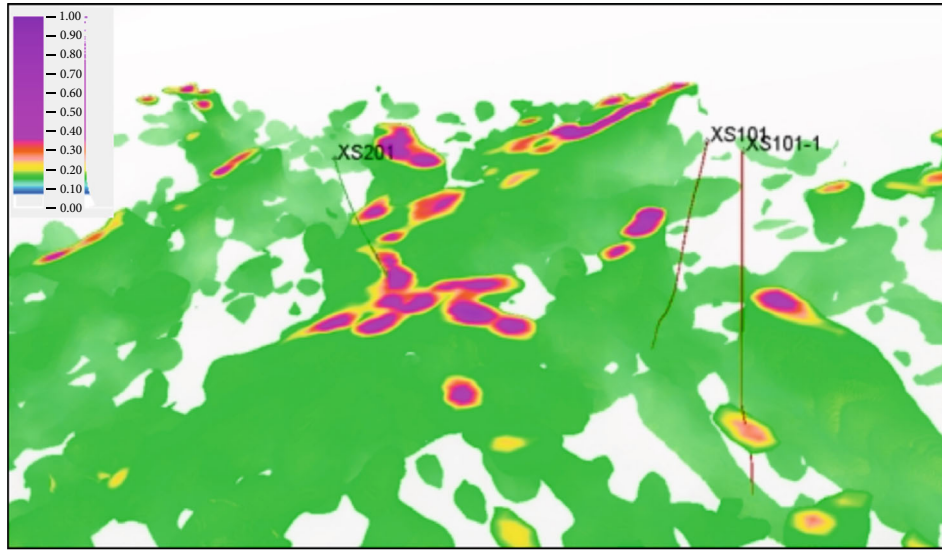


FIGURE 15: Fault-fracture reservoir model of the Xu 2 Member in the Xinchang area.

of TX₂¹ to TX₂⁸ in the Xu 2 Member. Then, these horizon data are further corrected with the geological stratification data from wells in this area. Finally, the corrected horizon data for each sand group are obtained. Petrel's model construction function in the structural modeling module is used to create the stratigraphic model of the Xu 2 Member in the Xinchang area (Figure 9).

Faults interpreted from conventional 3D seismic data are utilized to build the fault model using the deterministic method [31]. Fault interpretation on 3D seismic data is based on fault markers on the seismic section. As a result of this interpretation, the areal extension and occurrence of faults can be determined. The Xu 2 Member in the Xinchang area contains numerous faults with diversified assemblages, including step-like fault and Y-shaped fault. Given the complexity of the fault development in the Xu 2 Member, the first step in structural modeling is the fine characterization of relatively large-scale faults. With Petrel's fault framework function in the structural modeling module, seismic-interpreted fault data and fine-interpreted fault data are used as inputs to create the 3D fault geometry using the deterministic method and then build a refined 3D fault model (Figure 10).

Based on the horizon model and fault model, together with actual drilling data, the 3D structural model is constructed (Figure 11).

4.3.2. Fault-Dependent Natural Fracture Distribution Constraint Cube. As previously discussed in the paper. In particular, seismic attributes show good characterization effects near large-scale fault zones, while they have certain uncertainties in other areas. Likelihood and entropy cubes are extracted and then calibrated with artificially interpreted fault, and image log-interpreted fracture results to derive the range of values for each internal structure of the fault. Likelihood values of 0.15 to 1 define the sliding surface of the fault, and chaos (structure entropy) values of 0.18 to 1 for the sliding fracture zone and of 0.05 to 0.18 (Figure 12) are related to the induced fracture zone. Other values of the attribute are considered noise.

Likelihood and entropy integrated data cubes are extracted. With Petrel's attribute modeling function, the integrated data cube that characterizes the fault-dependent fractures is loaded into the structural model discussed in Section 3.1 to derive the fault-dependent natural fracture distribution constraint cube (Figure 13).

4.3.3. Construction of Discrete Fracture Network Model. Discrete fracture network modeling can really present the spatial distribution of fractures. With single-well image log-interpreted fracture density as the fundamental data and seismic attributes as constraints on the spatial distribution of fractures, such as likelihood and entropy that characterize the fault-dependent fractures and curvature that characterizes the fold-dependent fractures, Petrel's fracture modeling modulus is used to derive the fault-dependent natural fracture model for the study using the discrete fracture network modeling technique, under the control of the fisher distribution [32].

4.3.4. Interpretation of Fault-Fracture Reservoir Model. Based on the understandings stated above, the fault-fracture reservoir that represents the high-quality fractured gas reservoir is interpreted in 3D space to facilitate practical well placement. Petrel's geobody modulus is used for interpreting the likelihood-entropy integrated attribute cube (Figure 14).

4.3.5. Production Application Effect. The fault-fracture reservoir modeling technique stated above has been successfully applied to the development of the Xu 2 Member gas reservoir in the Xinchang area. Figure 15 shows the fault-fracture reservoir model derived from the integration of the entropy attribute that reflects the fault-dependent fractures and the likelihood attributes. Three wells, namely, XS201, XS101, and XS101-1, are deployed within the areas where the fault-fracture reservoir is present. The current gas production is $30 \times 10^4 \text{ m}^3/\text{d}$ from XS201, $15 \times 10^4 \text{ m}^3/\text{d}$ from XS101, and $20 \times 10^4 \text{ m}^3/\text{d}$ from XS101-1, much higher than any other well in the Xinchang area producing from the same pay zone. Thus, the fault-fracture reservoir interpretation and modeling technique provides powerful support for the development of a tight gas reservoir and can help optimize the well location and target for further development of tight gas.

5. Conclusions

- (1) The geological model of the fault-fracture reservoir in the Xu 2 Member in the Xinchang area includes the fault-fracture reservoir that is fault-dependent, the fold-fracture reservoir that is fold-dependent, and the fault-fold-fracture reservoir that is jointly controlled by fault and fold. The fault-fracture reservoir formed by the fault is dominant and widespread over the whole area
- (2) Likelihood and entropy attributes provide a useful tool to characterize the fault-fracture zone and the induced fracture zone. These attributes, as demonstrated by the image log and core data, yield a precise prediction of the fault-fracture reservoir in the Xu 2 Member in the Xinchang area
- (3) Under the guidance of the fault-dependent fracture geological model, geological information, well log data, and seismic attributes are integrated to characterize the fractures of different scales and determine the cutoff for each attribute to characterize the fault-fracture reservoir, and the fault-fracture model comprising natural fractures of different scales is constructed using the geological modeling technique. The geological model provides further guidance for the exploration and development of the Xu 2 Member tight gas reservoir in the Xinchang area. Encouraging drilling results have been reported

Data Availability

The original contributions presented in the study are included in the article; further inquiries can be directed to the corresponding author.

Conflicts of Interest

The authors declare that the research was conducted in the absence of any commercial or financial relationships that could be construed as a potential conflict of interest.

Acknowledgments

This research work is sponsored by Sinopec (34450000-21-ZC0607-0013).

References

- [1] J. Z. Li, B. C. Guo, M. Zheng, and T. Yang, "Main types, geological features and resource potential of tight sandstone gas in China," *Natural Gas Geoscience*, vol. 23, no. 4, pp. 607–615, 2012.
- [2] C. N. Zou, G. S. Zhang, Z. Yang et al., "Geological concepts, characteristics, resource potential and key techniques of unconventional hydrocarbon: on unconventional petroleum geology," *Petroleum Exploration and Development*, vol. 40, no. 4, pp. 385–399, 2013.
- [3] G. Q. Wei, F. D. Zhang, J. Li, S. Yang, C. Y. Huang, and Y. Q. She, "New progress of tight sand gas accumulation theory and favorable exploration zones in China," *Natural Gas Geoscience*, vol. 27, no. 2, pp. 199–210, 2016.
- [4] R. Wang, W. Ding, Y. Zhang et al., "Analysis of developmental characteristics and dominant factors of fractures in Lower Cambrian marine shale reservoirs: a case study of Niutitang Formation in Cen'gong block, southern China," *Journal of Petroleum Science and Engineering*, vol. 138, pp. 31–49, 2016.
- [5] R. Wang, G. Yang, W. Ding et al., "Characteristics and dominant controlling factors of organic-rich marine shales with high thermal maturity: a case study of the Lower Cambrian Niutitang Formation in the Cen'gong block, southern China," *Journal of Natural Gas Science and Engineering*, vol. 33, pp. 81–96, 2016.
- [6] C. Xiyuan, "Gas accumulation patterns and key exploration techniques of deep gas reservoirs in tight sandstone: an example from gas exploration in the Xujiahe Formation of the Western Sichuan Depression, the Sichuan Basin," *Oil & Gas Geology*, vol. 31, no. 6, pp. 707–714, 2010.
- [7] H. Huang, R. Li, F. Xiong et al., "A method to probe the pore-throat structure of tight reservoirs based on low-field NMR: Insights from a cylindrical pore model," *Marine and Petroleum Geology*, vol. 117, article 104344, 2020.
- [8] H. Huang, R. Li, Z. Jiang, J. Li, and L. Chen, "Investigation of variation in shale gas adsorption capacity with burial depth: insights from the adsorption potential theory," *Journal of Natural Gas Science and Engineering*, vol. 73, article 103043, 2020.
- [9] K. Zhang, C. Jia, Y. Song et al., "Analysis of lower Cambrian shale gas composition, source and accumulation pattern in different tectonic backgrounds: a case study of Weiyuan block in the upper Yangtze region and Xiuwu Basin in the lower Yangtze region," *Fuel*, vol. 263, article 115978, 2020.
- [10] K. Zhang, Y. Song, C. Jia et al., "Formation mechanism of the sealing capacity of the roof and floor strata of marine organic-rich shale and shale itself, and its influence on the characteristics of shale gas and organic matter pore development," *Marine and Petroleum Geology*, vol. 140, article 105647, 2022.
- [11] C. Fan, H. Xie, L. Hu et al., "Complicated fault characterization and its influence on shale gas preservation in the southern margin of the Sichuan Basin, China," *Lithosphere*, vol. 2022, no. Special 12, article 8035106, 2022.
- [12] J. Liu and D. Sun, "Tectono-stratigraphy and sedimentary infill characteristics of Xujiahe Formation in Western Sichuan foreland basin," in *AAPG International Conference and Exhibition, Cape Town, South Africa, 2015* <https://www.searchanddiscovery.com/abstracts/html/2018/ice2018/abstracts/2980967.html>.
- [13] L. Junlong, L. I. Zhongqun, X. I. Kaihua, Y. Huang, and J. I. Wujun, "Characterization of favorable lithofacies in tight sandstone reservoirs and its significance for gas exploration and exploitation: a case study of the 2nd member of Triassic Xujiahe Formation in the Xinchang area, Sichuan Basin," *Petroleum Exploration and Development*, vol. 47, no. 6, pp. 1194–1205, 2020.
- [14] R. Xie, W. Zhou, M. Xiang et al., "Development mode of reverse fault-associated fractures in deep tight sandstones: a case study in Xinchang gas field, Sichuan Basin, China," *Geological Journal*, vol. 56, no. 6, pp. 2997–3011, 2021.
- [15] M. S. Ameen, K. MacPherson, M. I. Al-Marhoon, and Z. Rahim, "Diverse fracture properties and their impact on performance in conventional and tight-gas reservoirs, Saudi Arabia: the Unayzah, South Haradh case study," *AAPG Bulletin*, vol. 96, no. 3, pp. 459–492, 2012.
- [16] L. Zeng, S. Hui, X. Tang, Y. Peng, and L. Gong, "Fractured tight sandstone oil and gas reservoirs: a new play type in the Dongpu Depression, Bohai Bay Basin, China," *AAPG Bulletin*, vol. 97, no. 3, pp. 363–377, 2013.
- [17] Z. Liu, Z. Liu, Y. Guo, Y. Ji, W. Li, and T. Lin, "Concept and geological model of fault-fracture reservoir and their application in seismic fracture prediction: a case study on the Xu2 member tight sandstone gas pool in Xinchang area, Western Sichuan Depression in Sichuan Basin," *Oil Gas Geology*, vol. 42, pp. 973–980, 2021.
- [18] Y. Zhang, L. Zeng, W. Lyu et al., "Natural fractures in tight gas sandstones: a case study of the upper Triassic Xujiahe Formation in Xinchang gas field, Western Sichuan Basin, China," *Geological Magazine*, vol. 158, no. 9, pp. 1543–1560, 2021.
- [19] L. Xiao, J. Li, Z. Mao, and Y. Hongyan, "A method to evaluate pore structures of fractured tight sandstone reservoirs using borehole electrical image logging," *AAPG Bulletin*, vol. 103, no. 1, pp. 205–226, 2020.
- [20] W. L. Ding, S. Yin, X. H. Wang, N. J. Zhang, M. Zhang, and X. Y. Cao, "Assessment method and characterization of tight sandstone gas reservoir fractures," *Earth Science Frontiers*, vol. 22, no. 4, pp. 173–187, 2015.
- [21] Z. Li, S. Liu, H. Chen, D. Sun, J. Lin, and C. Tang, "Structural superimposition and conjunction and its effects on hydrocarbon accumulation in the Western Sichuan Depression," *Petroleum Exploration and Development*, vol. 38, no. 5, pp. 538–551, 2011.
- [22] P. W. Wang, X. Chen, X. Q. Pang et al., "The controlling of structure fractures on the accumulation of tight sand gas reservoirs," *Natural Gas Geoscience*, vol. 25, no. 2, pp. 185–191, 2014.
- [23] H. Faqi, L. Chengchun, and L. Cheng, "Identification and description of fault-fracture bodies in tight and low permeability reservoirs in transitional zone at the south margin of Ordos Basin," *Oil & Gas Geology*, vol. 41, no. 4, pp. 710–718, 2020.
- [24] L. Micarelli, A. Benedicto, and C. A. J. Wibberley, "Structural evolution and permeability of normal fault zones in highly

- porous carbonate rocks,” *Journal of Structural Geology*, vol. 28, no. 7, pp. 1214–1227, 2006.
- [25] J. P. Evans, C. B. Forster, and J. V. Goddard, “Permeability of fault-related rocks, and implications for hydraulic structure of fault zones,” *Journal of Structural Geology*, vol. 19, no. 11, pp. 1393–1404, 1997.
- [26] Y. Gao, J. Zhang, H. Li, and G. Li, “Incorporating structural constraint into the machine learning high-resolution seismic reconstruction,” *IEEE Transactions on Geoscience and Remote Sensing*, vol. 60, pp. 1–12, 2022.
- [27] W. Wang and R. Fan, “Characteristics and exploration significance of “fault-fracture reservoirs” in the Xujiahe Formation, northern Sichuan Basin,” *Journal of Chengdu University of Technology: Science & Technology Edition*, vol. 46, no. 5, pp. 541–548, 2020.
- [28] T. Randen, E. Monsen, C. Signer et al., “Three-dimensional texture attributes for seismic data analysis,” *SEG Annual Meeting. OnePetro*, 2000.
- [29] Y. Luo, Y. E. Wang, N. M. AlBinHassan, and M. N. Alfaraj, “Computation of dips and azimuths with weighted structural tensor approach,” *Geophysics*, vol. 71, no. 5, pp. V119–V121, 2006.
- [30] A. A. Babasafari, G. F. Chinelatto, and A. C. Vidal, “Fault and fracture study by incorporating borehole image logs and supervised neural network applied to the 3D seismic attributes: a case study of pre-salt carbonate reservoir, Santos Basin, Brazil,” *Petroleum Science and Technology*, vol. 40, no. 12, pp. 1492–1511, 2022.
- [31] D. Hale, “Methods to compute fault images, extract fault surfaces, and estimate fault throws from 3D seismic images,” *Geophysics*, vol. 78, no. 2, pp. O33–O43, 2013.
- [32] L. V. Flataker, *A case study of usability design in ocean for petrel development at schlumberger information solutions*, [M.S. thesis], Institutt for Telematikk, 2009.